

# Highly efficient ‘hit-and-run’ genome editing with unconcentrated lentivectors carrying Vpr.Prot.Cas9 protein produced from RRE-containing transcripts

Ivana Indikova and Stanislav Indik<sup>✉\*</sup>

Institute of Virology, University of Veterinary Medicine Vienna, Veterinaerplatz 1, 1210 Vienna, Austria

Received December 04, 2019; Revised June 15, 2020; Editorial Decision June 17, 2020; Accepted June 25, 2020

## ABSTRACT

The application of gene-editing technology is currently limited by the lack of safe and efficient methods to deliver RNA-guided endonucleases to target cells. We engineered lentivirus-based nanoparticles to co-package the U6-sgRNA template and the CRISPR-associated protein 9 (Cas9) fused with a virion-targeted protein Vpr (Vpr.Prot.Cas9), for simultaneous delivery to cells. Equal spatiotemporal control of the *vpr.prot.cas9* and *gag/pol* gene expression (the presence of Rev responsive element, RRE) greatly enhanced the encapsidation of the fusion protein and resulted in the production of highly efficient lentivector nanoparticles. Transduction of the unconcentrated, Vpr.Prot.Cas9-containing vectors led to >98% disruption of the *EGFP* gene in reporter HEK293-EGFP cells with minimal cytotoxicity. Furthermore, we detected indels in the targeted endogenous loci at frequencies of up to 100% in cell lines derived from lymphocytes and monocytes and up to 15% in primary CD4+ T cells by high-throughput sequencing. This approach may provide a platform for the efficient, dose-controlled and tissue-specific delivery of genome editing enzymes to cells and it may be suitable for simultaneous endogenous gene disruption and a transgene delivery.

## INTRODUCTION

The scope and scalability of gene editing systems are currently limited by problems with the delivery of the CRISPR/Cas RNA-guided endonuclease (RGEN) components to recipient cells. Lipofection, electroporation, nucleofection and virus-based techniques are widely used to deliver CRISPR-associated protein 9 (Cas9)/single guide (sgRNA) expression cassettes. Unfortunately, the methods for delivering DNA have limited cell-type specificity and are associated with side effects, such as integration into undesired chromosomal locations, immunogenicity,

size-constrained packaging of expression cassettes (payload limit for AAV  $\leq 4.7$  kb) and increased off-targeting resulting from sustained expression. Increasing attention is thus being paid to the direct delivery of preassembled Cas9 protein/sgRNA complexes (RNPs) to cells (1,2), in which the rapid turnover of RNPs limits the exposure of the genome to nucleases, thereby mitigating off-target effects. Furthermore, the transient occurrence of RNPs in cells is expected to elicit minimal innate and adaptive immune responses, especially when a synthetic sgRNA lacking 5' triphosphates and a Cas9 orthologue derived from a species other than *Streptococcus pyogenes* are used (3,4). Despite the advantages of RNP delivery, the use of this approach is restricted to cell types that do not suffer from reduced cell viability or phenotypic changes following chemical transfection or electroporation. Furthermore, the technology requires laborious optimization of the transfection protocol for every cell type and lacks tissue and cell specificity. Thus, there is an urgent need for a more versatile, safe, cell-selective and ‘easy-to-use’ delivery system.

As a result of their efficiency, low toxicity, simplicity of production, mild immunogenicity, relative safety and ease of use and because of the possibility of customizing cell tropism, lentiviral vectors (LVs) are widely used in basic research and are being tested in numerous clinical trials for use in gene therapy (<http://www.abedia.com/wiley/index.html>) (5,6). Furthermore, LVs have recently been approved by the FDA for genetic engineering of T lymphocytes for cancer immunotherapy (7). In addition to nucleic acids, LVs can also deliver foreign proteins of interest (POIs) to mammalian cells (reviewed in (8)), and proof-of-concept studies have shown that LVs can serve as platforms for the administration of ‘protein-based’ designer nucleases to ablate host genes (9–12). However, the system suffers from modest effectiveness perhaps due to reduced infectivity of the viral particles containing structural proteins manipulated to make packaging of Cas9 protein possible. We now report engineered LVs with unmodified structural components that deliver the Cas9 protein together with a template for sgRNA in ‘all-in-one transducing nanoparticles’ and highly efficiently edit the targeted loci in the genome.

\*To whom correspondence should be addressed. Tel: +43 1 250772330; Email: stanislav.indik@vetmeduni.ac.at

## MATERIALS AND METHODS

### Cell lines, cell culture and quantification of EGFP-expressing cells

HEK293T (ATCC CRL-3216), HEK293 (ATCC CRL-1573), IM9 (CCL-159), SupT1 (CRL-1942), and Jurkat E6-1 (TIB-152) cell lines were obtained from ATCC. The THP-1 cells were obtained from Henning Hofmann (Robert Koch Institut). The human kidney cell lines were maintained in stable glutamine-containing high glucose Dulbecco's modified Eagle's medium (DMEM, Thermo Fisher Scientific) supplemented with 10% fetal bovine serum (FBS Gold Plus, Bio-Sell). The cell lines derived from human lymphocytes and monocytes were cultivated in stable glutamine-containing RPMI-1640 (Carl Roth) supplemented with 10% FBS Gold Plus (Bio-Sell). Cryopreserved Human CD4<sup>+</sup> T cells from normal human peripheral blood were acquired from Zen-Bio. More than 95% of the cells expressed CD3. The cells were cultured in X-VIVO 15 (Biozym) + 5% FBS Gold Plus (Bio-Sell) supplemented with IL-2 (100 ng/ml; PEPROTech) and IL-7 (15 ng/ml; PEPROTech). The cells were activated one day prior to transduction by adding Dynabeads Human T-cell activator CD3/CD28 (Thermo Fisher Scientific) at a bead to cell ratio of 1:1. For all cultivated cells, no antibiotics were used. The cells were maintained at 37°C and 5% CO<sub>2</sub> in a humidified incubator. To detect enhanced green fluorescent protein (EGFP)-positive cells, UV microscopy with the Olympus IX70 equipped with Olympus XM10 camera and CellSens software (Olympus) was used. 947 ms acquisition time was used to detect the HEK293-EGFP cells expressing a low-level of EGFP. To quantify the number of EGFP-positive cells, flow cytometry was performed. The cells were trypsinized, washed and analyzed using FACSCalibur flow cytometer and CellQuest Pro Software (BD Biosciences). Forward versus side scatter gating was used to approximate viable cell populations for analysis.

### Plasmid construction

A pVpr.Prot.Cas9 plasmid was constructed by Gibson assembly of a gBlock ordered from IDT (containing Vpr-, protease cleavage site-, and SV40 nuclear localization signal-coding sequence) and two PCR products containing Cas9 coding sequence and Rev-responsive element (RRE), respectively. The pLentiCRISPRv2 (a gift from F. Zhang; Addgene; plasmid #52961) was used as a template for the amplification of a DNA fragment encompassing the Cas9-coding sequence (13). The pCMgpRRE plasmid served as a template for the amplification of the DNA fragment containing RRE, CMV promoter,  $\beta$  globin polyA, and plasmid backbone sequence (14). A Vpr-coding region from the HIV-1 YU2 was used as a basis for the design of the gBlock sequence (15). The construct containing three copies of CTE in place of RRE (pVpr.Prot.Cas9-CTE3x) was constructed by Gibson assembly of two fragments generated by the high fidelity PCR (Q5, New England Biolabs). The long fragment contained sequence of the complete pVpr.Prot.Cas9 plasmid except the RRE-coding region. The short fragment, which was amplified using the 3-CTE3x plasmid as a template (16), contained 30 bp-long

overlapping ends. The pVpr.Prot.Cas9- (lacks RNA export elements) was constructed by re-ligating the long PCR fragment. A lentiviral transfer vector, Lenti(sgFILLER), which contains a filler sequence flanked by BsmBI sites in place of the 20 bp-long targeting crRNA sequence, was constructed from the pLentiCRISPRv2 by deleting Cas9-coding sequence in a long template PCR (primer pair: Fwd: 5'ATG ACC GAG TAC AAG CCC ACG3'; Rev: 5' CCT GTG TTC TGG CGG CAA AC 3') followed by circularization of the resulting PCR product. Lentiviral transfer vectors carrying sgRNAs targeting specific loci in the genome (Lenti(sgRNA)) were constructed from the Lenti(sgFILLER). The vector was digested with *BsmBI* and a pair of annealed and phosphorylated oligos was cloned into the single guide scaffold. D64V mutation was introduced into the psPAX2 plasmid by a high-fidelity PCR with a primer pair carrying the desired nucleotide substitution. Plasmids were amplified in DH5 $\alpha$  or NEB Stable competent *Escherichia coli* (New England Biolabs) and purified using a Qiagen Plasmid Midi kit (Qiagen).

### Lentivector production and transduction

To produce lentivectors containing both Cas9 protein and U6-sgRNA template five plasmids (a total amount of 4  $\mu$ g) were co-transfected to exponentially growing HEK293T cells seeded in six-well plates (ATCC CRL-3216; ~80% confluent) using Fugene HD (Promega). We used 1.2  $\mu$ g of transfer vector DNA (pLenti(sgRNA)), 0.9  $\mu$ g of psPAX2 (a gift from D. Trono; Addgene #12260) or psPAX2D64V, 0.6  $\mu$ g pRSV-Rev (a gift from D. Trono; Addgene #12253), 0.4  $\mu$ g of pHCMV-G (14), and 0.9  $\mu$ g of pVpr.Prot.Cas9. Transfection medium was replaced with fresh cell culture medium 20 h post-transfection. Virus-containing supernatants were harvested 48 h post-transfection, centrifuged (3500 rpm for 3 min), filtered (0.45  $\mu$ m, Sarstedt), and immediately used. For transduction of adherent cells, ~5  $\times$  10<sup>4</sup> cells were plated in each well of a 12-well plate one day before transduction. The plated cells were incubated with the virus-containing supernatant (350  $\mu$ l) supplemented with polybrene (8  $\mu$ g/ml) for 6 h. Then, 500  $\mu$ l of fresh cell culture medium (DMEM + 10% FBS Gold Plus) was added. For transduction of suspension cells, ~1  $\times$  10<sup>5</sup> cells in 50  $\mu$ l of cell culture medium were incubated with 100  $\mu$ l of virus-containing supernatant for 6 h. Next, cells were pelleted and re-suspended in fresh cell culture medium.

### Immunoblotting

The presence of viral and heterologous proteins in the cell lysates (cell, 10  $\mu$ g of total protein) and virions, harvested from cell culture supernatant 48 h after transfection (virus, 100 $\times$  concentrated by ultracentrifugation [20 000 g, 4°C, 2 h]), was determined by immunoblotting with antibodies specific for Cas9 protein ( $\alpha$ -Cas9 [mouse, 1:1000, 7A9-3A3; Cell Signalling Technology]). The HIV-1 proteins (p24 [CA] and Pr55 [Gag]) were detected following the re-probing of the membrane with an antibody raised against HIV-1 capsid protein ( $\alpha$ -HIV-1 p24, rabbit, 1:2000, a gift from Dr. Sakalian). As a loading control for cellular proteins, HSP90 was detected with an  $\alpha$ -HSP90 antibody (rabbit, 1:1000,

Cell Signalling Technology). The following secondary antibodies were used:  $\alpha$ -rabbit-IgG-HRP (1:10 000, DAKO, P0399) and  $\alpha$ -mouse-IgG-HRP (1:2000, DAKO, P0260). Chemiluminescent signal was detected with the SignalFire ECL Elite Substrate (Cell Signalling Technology). M: Protein Standard (NEB#P7712). Proteins in the SDS-PAGE gel were stained with Coomassie brilliant blue after blotting. Bands of interest were quantified by densitometry using ImageQuant TL software (GE Healthcare) and expressed as 'volume'.

### T7 endonuclease I assay

To detect genomic modification at the targeted regions, genomic DNA was extracted from transduced cells 3 days post-transduction using the Quick Extract DNA Extraction Solution (Lucigen) and used for PCR to amplify specific on-target sites with Phusion high fidelity DNA polymerase (New England Biolabs) and primer pairs specified in Supplementary data (list of oligos). PCR products were purified by Ampure XP beads (Beckman Coulter) according to the manufacturer's instructions. 200 ng of purified DNA were denatured and hybridized (95°C, 5 min; 95°C to 25°C,  $-0.1^\circ\text{C}/\text{s}$ ; hold at 4°C) in  $1 \times$  NEBuffer 2 (New England Biolabs) in a total volume of 14  $\mu\text{l}$ . 1  $\mu\text{l}$  of T7 Endonuclease I (New England Biolabs) was added to the hybridized PCR product and incubated at 37°C for 30 min. 5  $\mu\text{l}$  of 50% glycerol was added to the T7 Endonuclease reaction and 20  $\mu\text{l}$  was analyzed on a 2% agarose gel containing peqGREEN (VWR). The DNA band intensity was quantified using VisionWorks LS Analysis Software. The frequency of indel formation was calculated using the following equation:  $(1 - (1 - (b + c/a + b + c))^{1/2}) \times 100$ , where 'a' is the band intensity of DNA substrate and 'b' and 'c' are the cleavage products (17). It should be noted that we used this equation even though we are aware that it underestimates the editing efficiency in such a case that one type of editing predominates in a highly mutated locus as one mutant DNA duplex upon denaturation and re-annealing produces again mutant:mutant hybrid.

### High throughput sequencing and data analysis

For deep sequencing, genomic DNA from SupT1 and CD4+ T cells was prepared as described above. The genomic region flanking the targeted site was amplified in 20 cycles using Phusion high fidelity DNA polymerase (New England Biolabs) and the primer pairs specified in Supplementary data (list of oligos). The amplified sequences were purified (Ampure XP beads (Beckman Coulter)) and send for library preparation and sequencing on a MiSeq high-throughput sequencer ( $2 \times 300$  bp; Illumina) to LGC Genomics (Berlin). The 300 bp paired-end MiSeq raw reads were de-multiplexed and low quality reads (a PHRED quality score of  $<30$ ) removed using NextGen Sequence Workbench (Avalanche NextGen). The R1 and R2 fastq files were then uploaded to CRISPR Genome Analyzer (<http://crispr-ga.net/>) (18) together with the target sequence. The output figures and aligned indel-containing sequences flanking the cut site are shown in Supplementary Figures S29–S31. Deep sequencing data is available at the NCBI's Sequencing Read Archive (SRA).

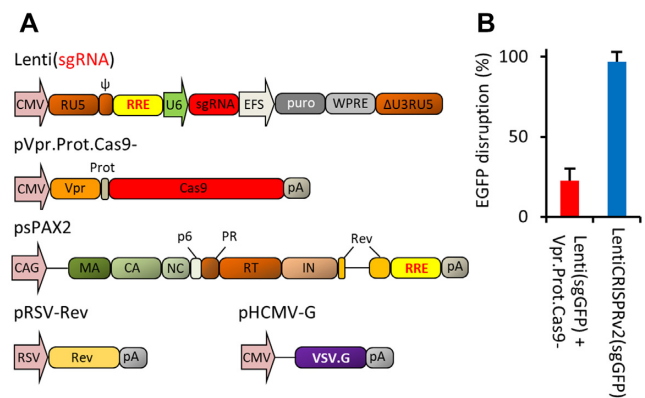


**Figure 1.** Delivery of the first generation of the two-component lentivector nanoparticles carrying the Cas9 nuclease protein and a template for the U6-sgRNA expression cassette (VECTR-Cas(sgGFP)) to human HEK293-EGFP cells. (A) Design of the constructs to generate the lentivector particles. Cas9 was fused to the C-terminus of Vpr containing an authentic HIV-1 protease cleavage site (CTLNF/PISPI; Vpr.Prot.Cas9). The U6-sgRNA expression cassette was incorporated into a lentiviral expression vector (Lenti(sgRNA)). The packaging construct (psPAX2) encodes the structural and enzymatic components of virions. The VSV.G envelope protein was used to pseudotype and stabilize viral particles (pHCMV-G). Efficient nuclear export and colocalization of mRNA for translation were supported by adding the Rev-responsive element (RRE) to the constructs and by overexpressing Rev during virion production (pRSV-Rev). Gag-Pol subunits: matrix (MA), capsid (CA), nucleocapsid (NC), p6, protease (PR), reverse transcriptase (RT) and integrase (IN). Packaging signal ( $\psi$ ); promoters (CMV, CAG, RSV, U6 and EFS), polyadenylation signal (pA), posttranscriptional regulatory element (WPRE). (B) The *EGFP* gene disruption in HEK293-EGFP cells after transduction with the first generation of the two-component lentivector (VECTR-Cas(sgGFP); red entry) or a control LentiCRISPRv2(sgGFP) (blue entry).

## RESULTS

### Nuclear export functions affect the packaging of Vpr.Prot.Cas9 protein into virions

We postulated that the large size ( $\sim 160$  kDa) and the net positive charge of Cas9 may cause structural disturbances and lead to reduced transducibility in such a case that the endonuclease is directly linked to the structural components of HIV-1 virions (embedded in the Gag polyprotein). To circumvent this problem, we fused Cas9 to the C-terminus of an accessory protein of HIV-1, Vpr, containing also an intervening protease cleavage site (Prot; Vpr.Prot.Cas9). Vpr interacts with the p6 domain of the Gag precursor, thereby mediating the encapsidation of its fusion partners into virions (19). To produce lentivector particles containing the Cas9 protein, the construct (pVpr.Prot.Cas9-) was co-transfected into HEK293T cells together with four complementary plasmids: (i) pHCMV-G, which produces the VSV.G envelope protein for pseudotyping virus particles; (ii) psPAX2, a second-generation packaging virus construct, which provides the virion proteins; (iii) pRSV-Rev, encoding Rev (We used additional Rev expression construct as the levels of Rev expressed from the packaging construct may be suboptimal (20)) and (iv) the pLenti(sgRNA) transfer vector containing a U6 promoter driving the expression of a sgRNA (in this case targeting the *EGFP* gene; sgGFP; Figure 1A). The resulting lentivector carrying the Cas9 protein and U6-sgGFP expression cassette (Vector for Combined

TRansduction of the Cas9 protein and U6-sgRNA; henceforth referred to as VECTR-Cas(sgRNA)) was transduced into the HEK293-EGFP cells containing a single copy of the *EGFP* reporter gene incorporated into chromosome 17 of the genome of HEK293 cells (Supplementary Figure S1). We used an EGFP disruption assay to determine whether the VECTR-Cas(sgGFP), produced from the transfected cells, can deliver the Cas9 protein to the nucleus of mammalian cells, form a complex with nascent sgRNA and induce mutagenesis. Transduction of the vector resulted only in a moderate EGFP disruption that contrasted with the high efficiency obtained with a potent *cas9* gene-delivering lentivector, LentiCRISPRv2(sgGFP) (Figure 1B; Supplementary Figure S2) (13). This result was consistent with previous work with meganucleases packaged into lentiviral particles with the help of Vpr that showed only a modest genome editing efficiency due to a low amount of the nuclease packaged into virions (9).

We hypothesized that we might be able to increase the packaging of foreign proteins fused to Vpr, including Vpr.Prot.Cas9, by directing the transport dynamics and/or spatial distribution of the *vpr.prot.cas9* transcripts. This assumption is based on earlier reports, which showed that the retroviral mRNA nuclear export elements regulate protein function and virion assembly (21–24). We imagined that if we direct the transcripts in the same manner as that of the *gag/pol* mRNA, which encodes the Gag polyprotein, we localize both transcripts to the same cytoplasmic microdomain for translation. Co-localization of the nascent Vpr.Prot.Cas9 and Gag proteins promotes their interaction and leads to enhanced encapsidation of the fusion protein into virions. To test this hypothesis, we constructed two Vpr.Prot.Cas9 expression constructs carrying various RNA export functions, pVpr.Prot.Cas9 (containing the Rev responsive element, RRE) and pVpr.Prot.Cas9-CTE<sub>3x</sub> (containing the constitutive transport element from MPMV, CTE; three copies of CTE were used to produce approximately the same levels of protein in the cytoplasm (16)) (Figure 2A). In the presence of Rev, the RRE facilitates mRNA export via the CRM1 pathway, whereas the CTE drives mRNA nuclear exit via the canonical NXF1 pathway (25–28). The constructs were co-transfected into HEK293T cells together with four complementary plasmids as shown in Figure 1. The amounts of Vpr.Prot.Cas9 produced in transfected cells and packaged into produced virions were determined by immunoblotting. As shown in Figure 2B, the levels of the fusion protein in the cell lysates of cells transfected with the two constructs were the same. In sharp contrast, the amount of Vpr.Prot.Cas9 packaged into virions increased by two-fold when the transcript contained the RRE (Figure 2B; Supplementary Figure S3). This result is consistent with a model in which the control of spatial localization and/or temporal distribution of transcripts encoding heterologous proteins affects the encapsidation of the proteins and it can be used to facilitate their packaging into virions (Figure 2C).

#### Highly efficient EGFP disruption with unconcentrated VECTR-Cas(sgGFP)

We used the EGFP disruption assay to determine whether the lentivector carrying Cas9 produced from the RRE-

containing transcript (VECTRv2-Cas(sgGFP)), ablates the *EGFP* gene more efficiently than the first generation lentivector, VECTR-Cas(sgGFP). Transduction of the unconcentrated VECTRv2-Cas(sgGFP) resulted in a robust loss of EGFP in ~90% of the EGFP-expressing cells (Figure 3A; Supplementary Figures S4A and S4B). Next, we optimized the amount of pVpr.Prot.Cas9 plasmid used to prepare VECTRv2-Cas(sgGFP). We observed the greatest extent of the *EGFP* gene disruption (~98%) with 0.9 µg of the construct in a total amount of 4 µg of transfected DNA (Supplementary Figure S5). The level of disruption was almost as high as that obtained with the *cas9* gene-delivering lentiviral vector pLentiCRISPRv2(sgGFP), which expresses large amounts of the Cas9 protein in target cells (13). Importantly, the level of EGFP expression was unchanged after transduction of a control lentivector lacking the Vpr.Prot.Cas9 protein or containing a sgRNA that targeted an *EMX1* locus (Figure 3A; Supplementary Figures S4A and B). No significant EGFP disruption was observed when the vector particles were prepared in the absence of the VSV.G envelope protein or when an inhibitor of reverse transcription, azidothymidine (AZT), was added to transduced cells (Figure 3A; Supplementary Figures S4A and B).

To confirm that the disruption of *EGFP* arose from genome modification and not from Cas9 binding or cellular toxicity, we measured the frequency of insertions/deletions (indels) at the target EGFP locus by means of a T7 endonuclease 1 (T7E1) assay and Inference of CRISPR Edits (ICE) analysis ([ice.synthego.com](http://ice.synthego.com)). Both assays revealed the presence of VECTRv2-Cas-induced double-strand breaks (DSBs) corrected by error-prone nonhomologous end joining (NHEJ). The frequencies of gene disruption differed (38% for T7E1 versus 97% for ICE) (Figure 3B and C; Supplementary Figure S6), perhaps due to a high frequency of +1 nt insertions (37% of indels) that increased the likelihood of reannealing the mutant DNA strands, leading to insensitivity of the resulting homoduplexes to T7E1 (Figure 3B and C; Supplementary Figure S6) (29). In contrast to transfection, transduction did not cause any appreciable toxicity in HEK293-EGFP cells, as validated by a Cell Proliferation assay (XTT) that showed only a minimal loss of cell viability after transduction (Supplementary Figure S7).

#### Highly efficient EGFP disruption with the integration deficient lentivector

The use of an integration-deficient vector would prevent the possibility of integrating lentiviral DNA, thereby improving the safety of two-component nanoparticles. Efficient knockouts mediated by programmable nucleases require only a short burst of activity, so we reasoned that the expression of sgRNAs from unintegrated viral DNA might be sufficient for gene ablation. We, therefore, tested the ability of vector particles containing a catalytically inactive integrase protein (D64V, VECTRv3-Cas(sgGFP)) (30) to disrupt EGFP. There was no detectable difference in gene ablation activity compared with that of the integration-proficient VECTRv2-Cas(sgGFP), indicating that the integration-deficient vector is a viable modification of the system (Figure 3D; Supplementary Figure S8).

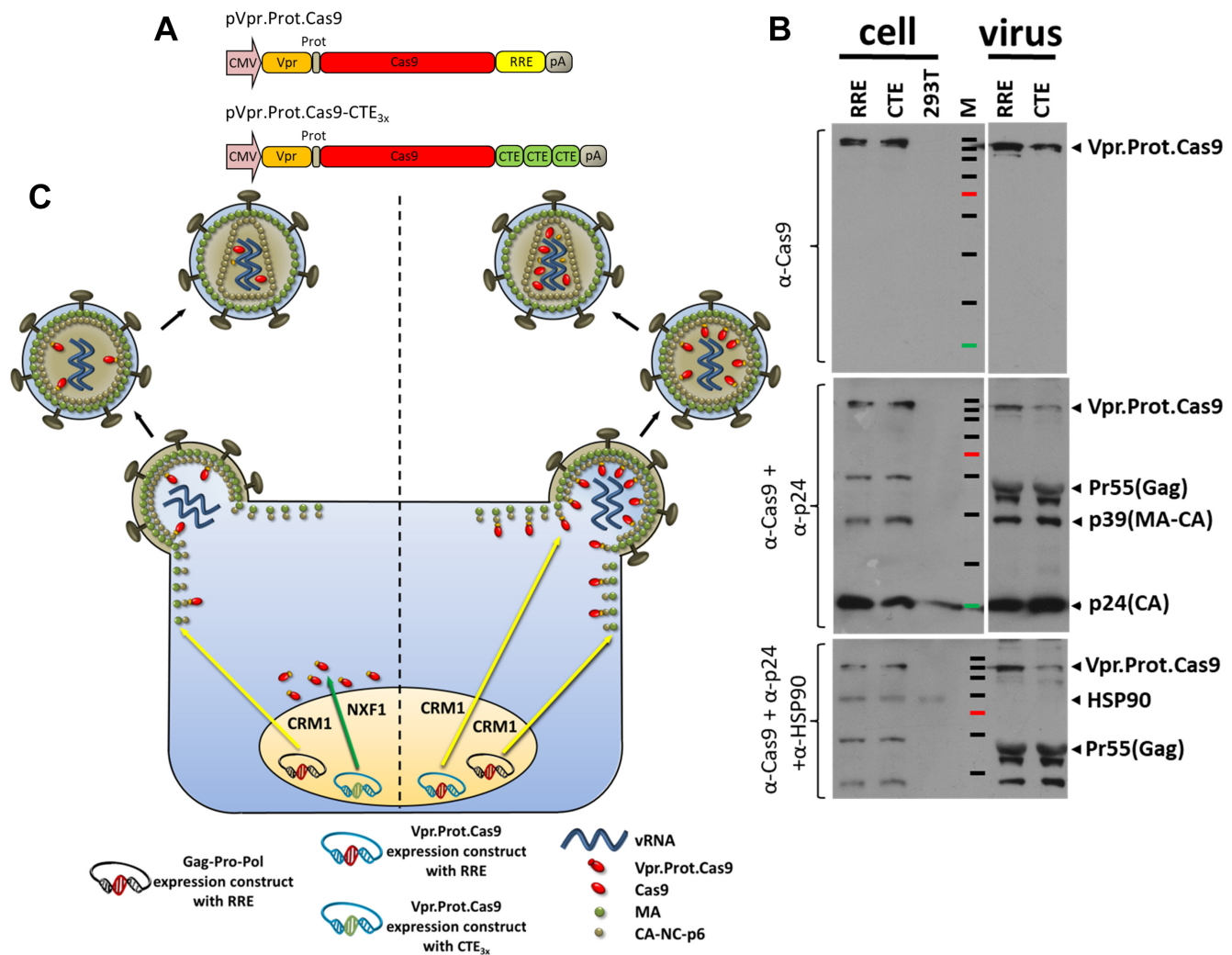


**Figure 2.** Enhanced packaging of the Vpr.Prot.Cas9 fusion protein produced from the transcript containing the Rev responsive element (RRE). (A) Schematic representation of the expression cassettes encoding Vpr.Prot.Cas9 fusion protein. The transcripts encoding Cas9 contain either the Rev responsive element (RRE) or the constitutive transport element (CTE). (B) The constructs were co-transfected into HEK293T cells together with psPAX2 (encodes structural and enzymatic components of virions from transcript containing the RRE) and with the other plasmids required for virus production as described in the Figure 1A. The presence of viral and heterologous proteins in the cell lysates (cell) and virions (virus) harvested from cell culture supernatant 48 h after transfection was determined by immunoblotting with antibodies as follows. The blot was probed with an antibody specific for the Cas9 protein. Next, the membrane was washed and re-probed with an antibody detecting the p24 (CA) and Pr55 (Gag) proteins to monitor the expression of the viral structural proteins in the lysates and to determine the amounts of virions released from transfected cells. Equivalent loading was confirmed by re-probing with an antibody directed against the HSP90 protein and by Coomassie blue staining of the SDS-PAGE gel after blotting. One representative example from three biological replicates performed in three different weeks is shown; 293T, untransfected cells; M, Color Prestained Standard NEB #P7712. (C) A model describing how nuclear export functions affect the packaging of heterologous proteins into virions. Retrovirus assembly and budding is a highly concerted process. It is mediated by numerous, largely undefined spatially and temporally regulated interactions between viral proteins and cellular factors. Previous reports showed that the regulation of the HIV-1 Gag assembly begins as soon as nuclear export factors are deposited onto the transcripts encoding the structural components of HIV-1. Here, we present a model whereby the selection of RNA export pathway modulates the cytosolic fate and function of the transcripts encoding heterologous proteins and facilitates the packaging of non-viral proteins into virions. The nuclear export of both viral and non-viral transcripts via the same pathway facilitates the cytoplasmic co-localization of the transcripts and their translation products. The close proximity of Gag and Vpr.Prot.Cas9 promotes the interaction between the two polyproteins that is required for encapsidation of the fusion protein into virions.

### Dose-controlled EGFP disruption

Transducing HEK293-EGFP cells with decreasing amounts of lentiviral vectors (LV) revealed a positive correlation between the dose of LV and the disruption of EGFP. The loss of knockout activity was more pronounced for the two-component VECTRv3-Cas(sgGFP) nanoparticles

than for the gene-delivering pLentiCRISPRv2(sgGFP), consistent with the idea that direct protein delivery is more vulnerable to a reduction of the effective nuclease protein concentration than is the administration of a nuclease gene expression cassette (Supplementary Figure S9).

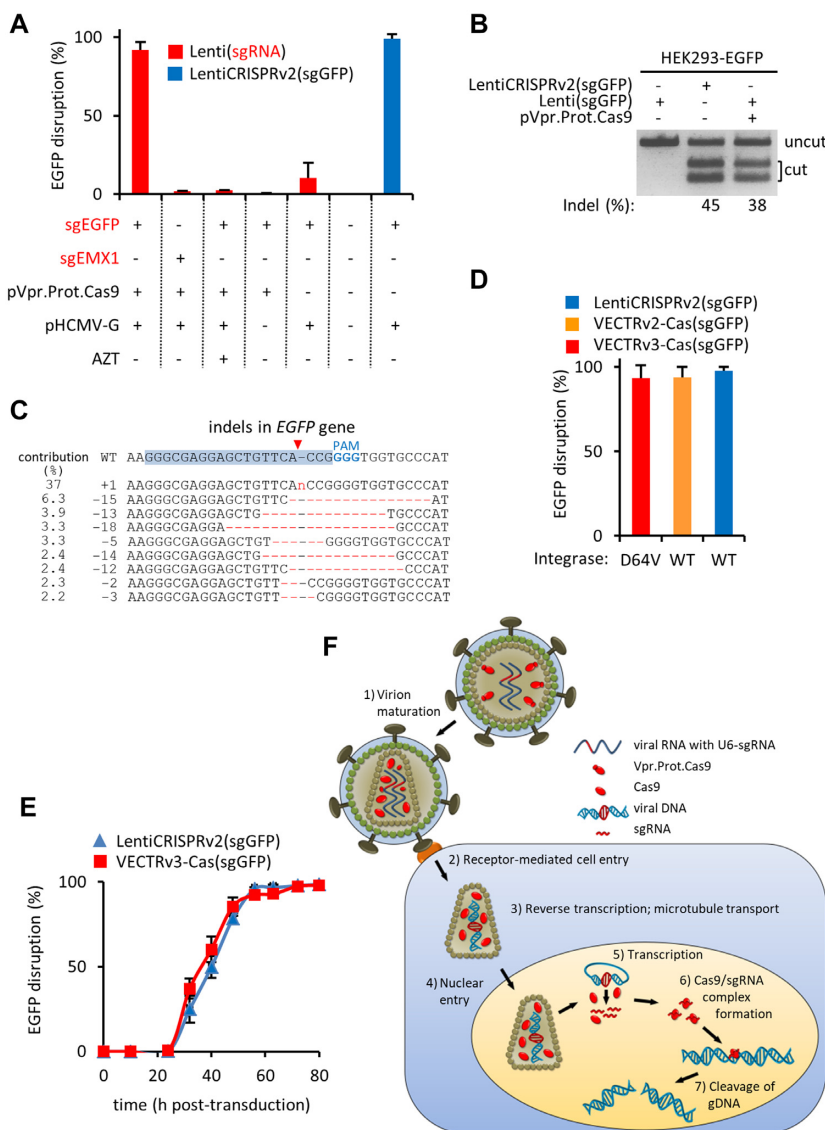


**Figure 3.** Delivery of the second (VECTRv2-Cas(sgGFP)) or third (VECTRv3-Cas(sgGFP)) generation of the two-component lentivector nanoparticles to human HEK293-EGFP cells. (A) The *EGFP* gene disruption in HEK293-EGFP cells after transduction with the second generation of the two-component lentivector (VECTRv2-Cas(sgGFP); red entries) or a control LentiCRISPRv2(sgGFP) (blue entry). (B) T7 endonuclease I (T7EI) assay to measure the indels in the *EGFP* gene resulting from transduction with the VECTRv2-Cas(sgGFP), the same vector lacking Vpr.Prot.Cas9 or a control vector pLentiCRISPRv2(sgGFP). The frequency of indel formation was calculated as described in the methods section. Please note that it may decrease the actual editing efficiency for highly efficient editing. (C) Mutant sequences at the *EGFP* locus and their frequencies, as determined by SYNTHOGO analysis of Sanger sequencing of a PCR product amplified from VECTRv2-Cas(sgGFP)-transduced HEK293-EGFP cells. The 20-nt target sequence is shown with a blue background. The protospacer adjacent motif (PAM) sequence is shown in blue. (D) Comparison of EGFP disruption after transduction with lentiviral particles containing integration-deficient (D64V; VECTRv3-Cas(sgGFP)) or integration-proficient (WT; VECTRv2-Cas(sgGFP)) integrase. (E) Time-course analysis of EGFP disruption mediated by the VECTRv3-Cas(sgGFP) or the gene-delivering LentiCRISPRv2(sgGFP). (F) A schematic representation of lentivector-mediated delivery of the Cas9 protein and viral RNA containing U6-sgRNA. Cas9 is packaged into virions as a Vpr.Prot.Cas9 fusion polyprotein that is proteolytically cleaved during virion maturation (1). Following virus entry into a recipient cell (2), the viral genome is reverse transcribed to DNA (3) and translocated to the nucleus together with Cas9 (4), where the U6 promoter drives the expression of sgRNA (5). The nascent sgRNA associates with Cas9 (6) and directs the nuclease to the target site in the genomic DNA (gDNA) for cleavage (7). (A, D) The mean activities of three replicates are shown. (E) The mean of two replicates are shown. (A, D, E) Error bars, mean  $\pm$  s.e.m.

### Time course of EGFP disruption following transduction with VECTRv3-Cas(sgGFP) or pLentiCRISPRv2(sgGFP)

We compared the kinetics of EGFP disruption between VECTRv3-Cas(sgGFP) and pLentiCRISPRv2(sgGFP) by following the expression of EGFP over an 80 h period after transduction. There was no difference in the time course of

gene disruption. Both RNA-guided endonuclease (RGEN) delivery methods required a lag period of over 24 h to disrupt EGFP, which was followed by a steady increase in disruption, plateauing at 56 h post-transduction (Figure 3E; Supplementary Figure S10A). The loss of fluorescence remained stable over a period of 35 days after treatment (Supplementary Figure S10B). In combination with the findings

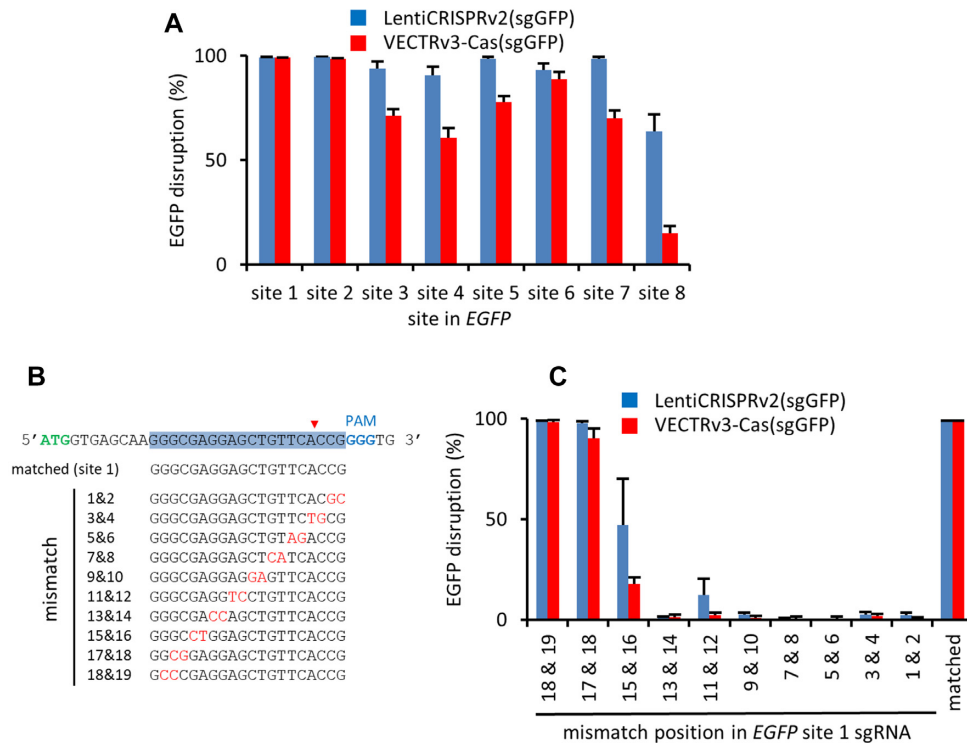


**Figure 4.** (A) EGFP disruption activity of the two lentivectors directed to different sites within the *EGFP* gene. (B) The positioning of mismatched bases in each sgRNA targeted to *EGFP* site 1. The EGFP start codon is shown in green. (C) Double mismatch tolerance of the two-component VECTrv3-Cas(sgGFP) vs. LentiCRISPRv2(sgGFP) harboring variant mismatched sgRNAs. A matched sgRNA for site 1 was used as a control. (A, C) The mean activities of three replicates are shown. Error bars, mean  $\pm$  s.e.m.

obtained with AZT, which indicated that reverse transcription is required for site-specific mutagenesis (Figure 3A), these results support a model in which a complex between Cas9 and sgRNA is formed in the nucleus of the recipient cells rather than during the assembly of viral particles (Figure 3F).

### EGFP disruption with sgRNAs targeting various sites in the *EGFP* gene

To ensure that disruption of EGFP is not a peculiarity of the sgRNA used (sgGFP site No. 1), we tested the activity of a set of *EGFP*-targeting sgRNAs (sgGFP site Nos. 28). One of these sgRNAs (targeting site No. 2) induced indels with a frequency comparable to that mediated by the original sgRNA. The remaining six sgRNAs yielded mutation rates that ranged from 12% to 85% (Figure 4A; Supplementary Figure S11). The gene delivery vectors consistently exhibited more robust editing activity than the vectors that directly transferred the Cas9 protein, although the magnitude of the difference was not the same for all sites. The effect was particularly salient for the sgRNA that targeted site No. 8, which was the least edited site (Figure 4A; Supplementary Figure S11). It appears that some of the targeted loci are more sensitive to changes in Cas9/sgRNA concentrations in the cell and thus that the design of the sgRNAs is particularly important for systems that directly deliver RGENs to cells.

### VECTrv3-Cas9(sgRNA) is more specific than *cas9* gene-transducing lentivector

Next, we investigated whether the VECTrv3-Cas(sgRNA) system is more sensitive than the lentivirus-mediated administration of nucleic acids, to Watson-Crick mismatches at the sgRNA–DNA interface. We determined the EGFP disruption activity of both lentivirus-based delivery systems bearing variants of the original sgRNA (sgGFP site No. 1) with adjacent double mismatches at positions 1–19 (numbered in the 3' to 5' direction; Figure 4B). Regardless of the route of RGEN administration, the EGFP disruption activity was robust and equivalent to that mediated by the matched sgRNA when the sgRNA contained mismatches at positions 17&18 and 18&19. The sgRNA containing mismatches at position 15&16 yielded less potent editing than the matched sgRNA, and the loss of activity was more dramatic when the sgRNA was transduced into cells together with the Cas9 protein. Of the remaining seven sgRNAs, only sgGFP(11&12) showed appreciable activity and only when delivered via the pLentiCRISPRv2 encoding the nuclease (Figure 4C; Supplementary Figure S12). These results are consistent with reports that mismatches at the 5' end of sgRNAs are better tolerated than those at the 3' end and establish that VECTrv3-Cas-mediated editing is more specific than mutagenesis induced by the transduction of the *cas9* gene into cells (31,32).

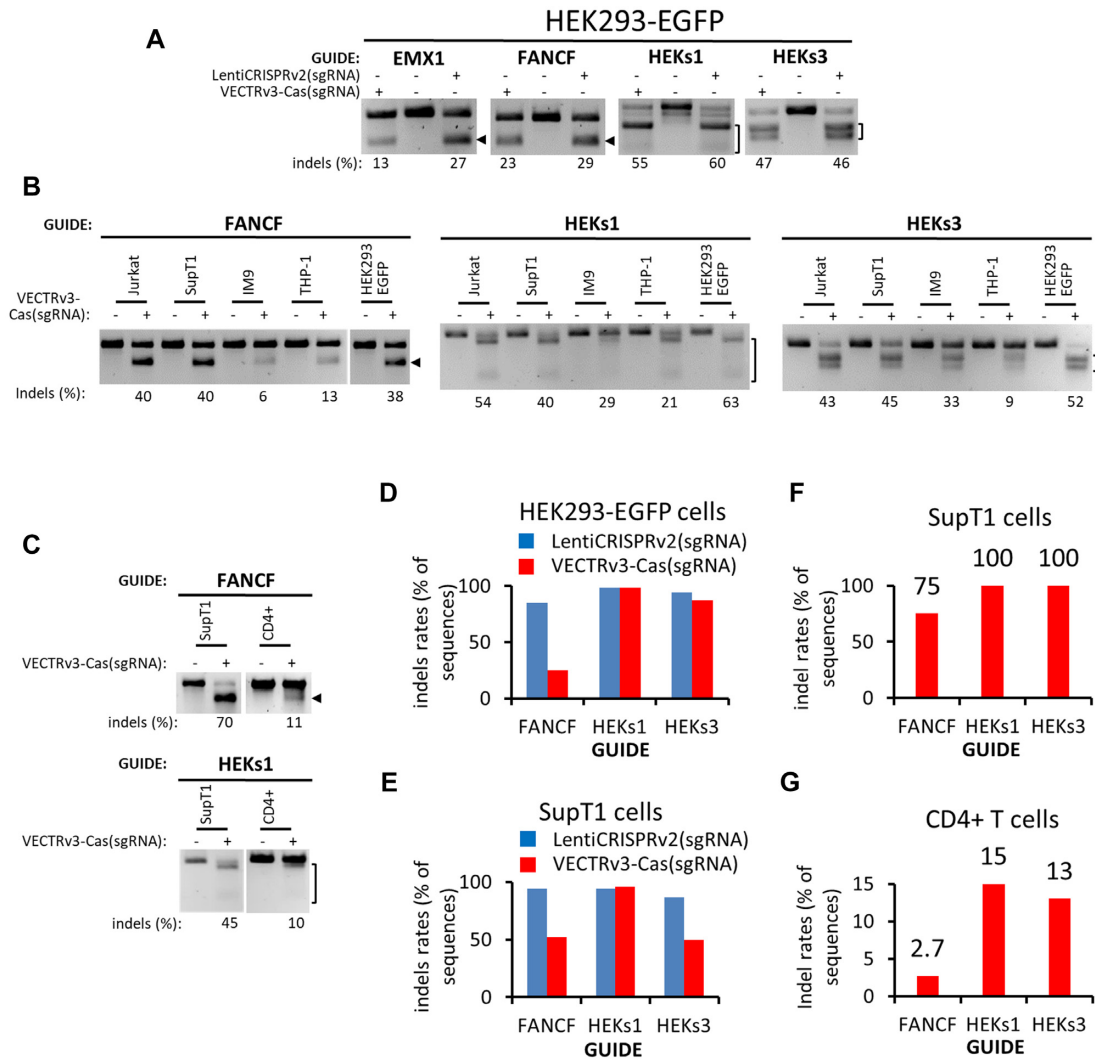


**Figure 5.** VECTRv3-Cas(sgRNA)-mediated genome editing of the native loci in multiple cell types. (A) Detection of indels by a T7E1 assay in the endogenous EMX1, FANCF, HEKs1 and HEKs3 loci in HEK293-EGFP cells transduced with VECTRv3-Cas(sgRNA) or LentiCRISPRv2(sgRNA). The frequency of indel formation was calculated as described in the methods section. Please note that it may decrease the actual editing efficiency for highly efficient editing. (B) VECTRv3-Cas(sgRNA)-mediated mutation of the FANCF, HEKs1 and HEKs3 loci in lines of human T lymphocytes (Jurkat, SupT1), B lymphocytes (IM9) and monocytes (THP-1) measured with the T7E1 assay. Mutation rates obtained from parallel transductions of HEK293-EGFP cells are also shown. (C) The indel rates (measured by the T7E1 assay) in primary CD4+ T cells transduced with VECTRv3-Cas(sgRNA). The parallel transduction of SupT1 cells served as a positive control. Please note that the HEKs3 site could not be analyzed by the T7E1 assay due to single-nucleotide polymorphism (SNP) near the cut site (Supplementary Figure S31). (D, E) Indel frequencies quantified by the ICE (Synthego) using Sanger sequencing data, generated from amplicons, as an input. The HEK293-EGFP (D) were transduced in parallel with SupT1 (E) using either VECTRv3-Cas(sgRNA) (red) or LentiCRISPRv2(sgRNA) (blue) targeted to the specific locus (FANCF, HEKs1, HEKs3). (Supplementary Figures S17–28). (F, G) Indel frequencies quantified by the CRISPR Genome Analyzer using the next-generation sequencing data of amplicons from (C) as an input (18). (F) SupT1 T cell line; (G) primary CD4+ T cells (Supplementary Figures S29–S31).

### Ablation of the endogenous genes in cell lines and primary lymphocytes

To test whether virions delivering Cas9 protein:template sgRNA can induce the cleavage of endogenous genes in human cells, we transduced HEK293-EGFP cells with VECTRv3-Cas(sgRNA) targeted to the EMX1, FANCF, HEKs1 and HEKs3 loci in the human genome. The T7E1 assay revealed that indels formed at all four genomic loci with efficiencies similar to those achieved with *cas9* gene-delivering virions (1355%) (Figure 5A). The ICE analysis of amplicons obtained from

the HEKs1 locus showed a high mutation efficiency of 99% and 97% for VECTRv3-Cas(sgHEKs1) and LentiCRISPRv2(sgHEKs1), respectively (Supplementary Figures S13 and S14). The VECTRv3-Cas(sgRNA) can also induce site-specific double-strand breaks in more technically challenging cell types, including the Jurkat E6-1 (T cell leukemia), SupT1 (T cell lymphoma), IM9 (B lymphoblastoid), and THP-1 (acute monocytic leukemia) cell lines, as well as primary CD4+ T cells. Indels formed at frequencies ranging from 6% to 70% in all cell types tested as determined by the T7E1 assay (Figure 5B and C; Supplementary Figures S15 and S16). IM9, THP-1, and CD4+ T cells

were less edited, but the two T cell-derived lines, Jurkat and SupT1, were as sensitive to the induction of mutations as HEK293-EGFP cells.

Next, we compared the indel formation frequencies induced by VECTRv3-Cas(sgRNA) and LentiCRISPRv2(sgRNA), respectively, in SupT1 and HEK293-EGFP cells. The ICE analysis revealed only a moderately decreased indel formation frequencies in both cell lines transduced with the Cas9 protein-delivering lentivectors targeting the HEKsite1 and HEKsite3 loci (averaging  $82.8 \pm 22.4\%$  for VECTRv3-Cas(sgHEKs1) and VECTRv3-Cas(sgHEKs3) versus  $93.3 \pm 4.6\%$  for LentiCRISPRv2(sgHEKs1) and LentiCRISPRv2(sgHEKs3)) (Figure 5D and E; Supplementary Figures S17–S24). The reduction of gene disruption was more pronounced for the FANCF locus. The mutation frequency averaged  $38.5 \pm 19.1\%$  for VECTRv3-Cas(sgFANCF), while indel formation averaged  $89.5 \pm 6.4\%$  for LentiCRISPRv2(sgFANCF) (Figure 5D and E; Supplementary Figures S25–S28).

Finally, we used amplicons generated with genomic DNA from SupT1 and CD4+ T cells for high-throughput sequencing to verify and quantify on-target mutations at the FANCF, HEKs1, and HEKs3 loci. For CD4+ cells, we found indels at frequencies of  $\sim 3\%$ ,  $15\%$  and  $13\%$ , respectively, while transduction of SupT1 yielded cleavage efficiencies of  $75\%$ ,  $100\%$  and  $100\%$ , respectively (Figure 5F and G; Supplementary Figures S29–S31).

## DISCUSSION

Here, we describe a novel system for the codelivery of the Cas9 protein and a template for sgRNA within lentivirus-based ‘nanoparticles’. The idea is built upon findings that lentiviruses can simultaneously deliver foreign proteins and an episomal viral DNA generated by reverse transcription from the vector RNA genome (9,10). We have extended this approach to show that episomal DNA can serve as a template for the transcription of sgRNA, which forms a complex with the co-delivered Cas9 protein and targets the nuclease to a specific site in the genome. This strategy leads to robust editing activity that appears to be comparable or even superior to that reported for the direct delivery of Cas9 protein/sgrNA complexes to cells (1,2). In contrast to chemical transfection or electroporation, virus-mediated delivery is receptor-mediated, so the use of pseudotypes bearing natural or engineered envelope proteins would allow selective transfer to essentially any target cell population (6). This approach may even extend the repertoire of cell types that can be edited to clinically relevant nondividing cells (e.g. neurons, hepatocytes, quiescent lymphocytes, and hematopoietic stem cells) that are permissive for the lentivector-mediated transduction of cargos to the nucleus (5). Additionally, because the removal of *cas9* transgene from the lentiviral transfer vector makes space for additional function-conferring elements, we imagine that the approach can be developed to a multiple-component system for simultaneous knock-out and delivery of genes. For example, simultaneous disruption of the T cells receptor (TCR) and delivery of the chimeric artificial receptor (CAR) may simplify the development and manufacturing of

the advanced medicinal products such as allogeneic CAR-T cells.

To our knowledge, this is the first study that uses the unconcentrated lentivector preparations for highly efficient genome editing. There are several possible explanations for the high efficiency of the two-component VECTRv2/3-Cas nanoparticles. First, we fused Cas9 to Vpr rather than to the Gag polyprotein, as we anticipated that the incorporation of the bulky nuclease into Gag would destabilize the virions and lower the efficiency of transduction. Second, we incorporated the RRE into the transcripts encoding Gag and Vpr.Prot.Cas9 proteins, providing simultaneous control of transport and spatial distribution to both mRNAs and resulting in the accumulation of Vpr.Prot.Cas9 in viral particles (21,22). This probably results from the colocalization of nascent Gag and Vpr.Prot.Cas9 proteins after translation, facilitating the interaction between p6 (in Gag) and Vpr (in Vpr.Prot.Cas9) and stimulating the incorporation of the fusion protein into virions (Figure 2C). Alternatively, analogous post-transcriptional regulation of gene expression might have allowed the interaction with a cellular factor responsible for the trafficking of transcripts and/or proteins to the virus assembly site. Third, the Cas9 protein remains embedded in a lentiviral core after receptor-mediated cell entry (where it is protected from degradation) and exploits viral intracellular trafficking routes to travel to the nucleus. Finally, the coordinated intranuclear delivery of Cas9 and viral DNA within a preintegration complex particle probably places the nuclease in close proximity to nascent sgRNA molecules synthesized from viral DNA, facilitating the formation of Cas9/sgrNA RNP complexes (Figure 3F).

In summary, we describe novel multicomponent lentiviral nanoparticles that ferry the Cas9 protein:sgRNA template to the nuclei of transduced cells for the transient exposure of the genome to the nuclease that results in the specific and highly efficient disruption of targeted loci. This system may represent a versatile platform for the efficient, safe, non-toxic and cell type-selective delivery of genome modification enzymes to cells.

## DATA AVAILABILITY

Raw MiSeq sequencing files are publicly available at the European Nucleotide Archive (ENA; [www.ebi.ac.uk/ena](http://www.ebi.ac.uk/ena)) under accession number: PRJEB32556.

## SUPPLEMENTARY DATA

Supplementary Data are available at NAR Online.

## ACKNOWLEDGEMENTS

We thank M. Sakalian for generously providing the p24-specific antibody and H. Hofmann for the THP-1 cells. The funders had no role in study design, data collection and analysis, decision to publish, or preparation of the manuscript.

## FUNDING

Austrian Science Fund (FWF) [P24577 to S.I.]. Funding for open access charge: Austrian Science Fund [P24577].

**Conflict of interest statement.** A patent related to this work is pending.

## REFERENCES

- Zuris, J.A., Thompson, D.B., Shu, Y., Guilinger, J.P., Bessen, J.L., Hu, J.H., Maeder, M.L., Joung, J.K., Chen, Z.Y. and Liu, D.R. (2015) Cationic lipid-mediated delivery of proteins enables efficient protein-based genome editing in vitro and in vivo. *Nat. Biotechnol.*, **33**, 73–80.
- Kim, S., Kim, D., Cho, S.W., Kim, J. and Kim, J.S. (2014) Highly efficient RNA-guided genome editing in human cells via delivery of purified Cas9 ribonucleoproteins. *Genome Res.*, **24**, 1012–1019.
- Wagner, D.L., Amini, L., Wendering, D.J., Burkhardt, L.M., Akyuz, L., Reinke, P., Volk, H.D. and Schmuck-Henneresse, M. (2018) High prevalence of *Streptococcus pyogenes* Cas9-reactive T cells within the adult human population. *Nat. Med.*, **25**, 242–248.
- Kim, S., Koo, T., Jee, H.G., Cho, H.Y., Lee, G., Lim, D.G., Shin, H.S. and Kim, J.S. (2018) CRISPR RNAs trigger innate immune responses in human cells. *Genome Res.*, **28**, 367–373.
- Naldini, L., Blomer, U., Gallay, P., Ory, D., Mulligan, R., Gage, F.H., Verma, I.M. and Trono, D. (1996) In vivo gene delivery and stable transduction of nondividing cells by a lentiviral vector. *Science*, **272**, 263–267.
- Anliker, B., Abel, T., Kneissl, S., Hlavaty, J., Caputi, A., Brynza, J., Schneider, I.C., Munch, R.C., Petznek, H., Kontermann, R.E. et al. (2010) Specific gene transfer to neurons, endothelial cells and hematopoietic progenitors with lentiviral vectors. *Nat. Methods*, **7**, 929–935.
- Mullard, A. (2017) FDA approves first CAR T therapy. *Nat. Rev. Drug Discov.*, **16**, 669.
- Cai, Y. and Mikkelsen, J.G. (2014) Driving DNA transposition by lentiviral protein transduction. *Mob. Genet. Elem.*, **4**, e29591.
- Izmiryan, A., Basmaciogullari, S., Henry, A., Paques, F. and Danos, O. (2011) Efficient gene targeting mediated by a lentiviral vector-associated meganuclease. *Nucleic Acids Res.*, **39**, 7610–7619.
- Cai, Y., Bak, R.O. and Mikkelsen, J.G. (2014) Targeted genome editing by lentiviral protein transduction of zinc-finger and TAL-effector nucleases. *eLife*, **3**, e01911.
- Choi, J.G., Dang, Y., Abraham, S., Ma, H., Zhang, J., Guo, H., Cai, Y., Mikkelsen, J.G., Wu, H., Shankar, P. et al. (2016) Lentivirus pre-packed with Cas9 protein for safer gene editing. *Gene Ther.*, **23**, 627–633.
- Lyu, P., Javidi-Parsijani, P., Atala, A. and Lu, B. (2019) Delivering Cas9/sgRNA ribonucleoprotein (RNP) by lentiviral capsid-based bionanoparticles for efficient 'hit-and-run' genome editing. *Nucleic Acids Res.*, **47**, e99.
- Sanjana, N.E., Shalem, O. and Zhang, F. (2014) Improved vectors and genome-wide libraries for CRISPR screening. *Nat. Methods*, **11**, 783–784.
- Konstantoulas, C.J. and Indik, S. (2014) Mouse mammary tumor virus-based vector transduces non-dividing cells, enters the nucleus via a TNPO3-independent pathway and integrates in a less biased fashion than other retroviruses. *Retrovirology*, **11**, 34.
- Wu, X., Liu, H., Xiao, H., Kim, J., Seshiah, P., Natsoulis, G., Boeke, J.D., Hahn, B.H. and Kappes, J.C. (1995) Targeting foreign proteins to human immunodeficiency virus particles via fusion with Vpr and Vpx. *J. Virol.*, **69**, 3389–3398.
- Wodrich, H., Schambach, A. and Krausslich, H.G. (2000) Multiple copies of the Mason-Pfizer monkey virus constitutive RNA transport element lead to enhanced HIV-1 Gag expression in a context-dependent manner. *Nucleic Acids Res.*, **28**, 901–910.
- Ran, F.A., Hsu, P.D., Wright, J., Agarwala, V., Scott, D.A. and Zhang, F. (2013) Genome engineering using the CRISPR-Cas9 system. *Nat. Protoc.*, **8**, 2281–2308.
- Guell, M., Yang, L. and Church, G.M. (2014) Genome editing assessment using CRISPR Genome Analyzer (CRISPR-GA). *Bioinformatics*, **30**, 2968–2970.
- Paxton, W., Connor, R.I. and Landau, N.R. (1993) Incorporation of Vpr into human immunodeficiency virus type 1 virions: requirement for the p6 region of gag and mutational analysis. *J. Virol.*, **67**, 7229–7237.
- Ikeda, Y., Takeuchi, Y., Martin, F., Cosset, F.L., Mitrophanous, K. and Collins, M. (2003) Continuous high-titer HIV-1 vector production. *Nat. Biotechnol.*, **21**, 569–572.
- Pocock, G.M., Becker, J.T., Swanson, C.M., Ahlquist, P. and Sherer, N.M. (2016) HIV-1 and M-PMV RNA nuclear export elements program viral genomes for distinct cytoplasmic trafficking behaviors. *PLoS Pathog.*, **12**, e1005565.
- Swanson, C.M., Puffer, B.A., Ahmad, K.M., Doms, R.W. and Malim, M.H. (2004) Retroviral mRNA nuclear export elements regulate protein function and virion assembly. *EMBO J.*, **23**, 2632–2640.
- Sherer, N.M., Swanson, C.M., Papaioannou, S. and Malim, M.H. (2009) Matrix mediates the functional link between human immunodeficiency virus type 1 RNA nuclear export elements and the assembly competency of Gag in murine cells. *J. Virol.*, **83**, 8525–8535.
- Jin, J., Sturgeon, T., Chen, C., Watkins, S.C., Weisz, O.A. and Montelaro, R.C. (2007) Distinct intracellular trafficking of equine infectious anemia virus and human immunodeficiency virus type 1 Gag during viral assembly and budding revealed by bimolecular fluorescence complementation assays. *J. Virol.*, **81**, 11226–11235.
- Braun, I.C., Rohrbach, E., Schmitt, C. and Izaurralde, E. (1999) TAP binds to the constitutive transport element (CTE) through a novel RNA-binding motif that is sufficient to promote CTE-dependent RNA export from the nucleus. *EMBO J.*, **18**, 1953–1965.
- Fornerod, M., Ohno, M., Yoshida, M. and Mattaj, I.W. (1997) CRM1 is an export receptor for leucine-rich nuclear export signals. *Cell*, **90**, 1051–1060.
- Fukuda, M., Asano, S., Nakamura, T., Adachi, M., Yoshida, M., Yanagida, M. and Nishida, E. (1997) CRM1 is responsible for intracellular transport mediated by the nuclear export signal. *Nature*, **390**, 308–311.
- Stade, K., Ford, C.S., Guthrie, C. and Weis, K. (1997) Exportin 1 (Crm1p) is an essential nuclear export factor. *Cell*, **90**, 1041–1050.
- Kim, J.M., Kim, D., Kim, S. and Kim, J.S. (2014) Genotyping with CRISPR-Cas-derived RNA-guided endonucleases. *Nat. Commun.*, **5**, 3157.
- Leavitt, A.D., Robles, G., Alesandro, N. and Varmus, H.E. (1996) Human immunodeficiency virus type 1 integrase mutants retain in vitro integrase activity yet fail to integrate viral DNA efficiently during infection. *J. Virol.*, **70**, 721–728.
- Fu, Y., Foden, J.A., Khayter, C., Maeder, M.L., Reyon, D., Joung, J.K. and Sander, J.D. (2013) High-frequency off-target mutagenesis induced by CRISPR-Cas nucleases in human cells. *Nat. Biotechnol.*, **31**, 822–826.
- Hsu, P.D., Scott, D.A., Weinstein, J.A., Ran, F.A., Konermann, S., Agarwala, V., Li, Y., Fine, E.J., Wu, X., Shalem, O. et al. (2013) DNA targeting specificity of RNA-guided Cas9 nucleases. *Nat. Biotechnol.*, **31**, 827–832.